Supporting Information

Chiral crystallization and optical properties of three metal complexes based on two non-centrosymmetric tripodal ligands †

Ming-Dao Zhang,[a,b] Zhi-Qiang Shi,[b] Min-Dong Chen,[a] and He-Gen Zheng*,[b]

[a] *Jiangsu Key Laboratory of Atmospheric Environment Monitoring and Pollution Control, Collaborative Innovation Center of Atmospheric Environment and Equipment Technology, School of Environmental Science and Engineering, Nanjing University of Information Science & Technology, Nanjing 210044, P. R. China.*
[b] *State Key Laboratory of Coordination Chemistry, School of Chemistry and Chemical Engineering, Nanjing National Laboratory of Microstructures, Nanjing University, Nanjing 210093, P. R. China.*

Table S1. Selected Bond Lengths (Å) and Angles (deg) for Complexes **1-3**.

Complex **1**			
Cd3–O4	2.267(2)	Cd3–N1	2.306(3)
Cd3–N3	2.320(3)	Cd3–O1#1	2.349(2)
Cd3–N2	2.355(3)	Cd3–O2#1	2.471(2)
O4–Cd3–N1	89.07(10)	O4–Cd3–N3	137.22(10)
N1–Cd3–N3	92.55(10)	O4–Cd3–O1#1	135.06(9)
N1–Cd3–O1#1	92.45(10)	N3–Cd3–O1#1	87.60(10)
O4–Cd3–N2	85.22(10)	N1–Cd3–N2	174.03(10)
N3–Cd3–N2	92.84(10)	O1#1–Cd3–N2	90.36(9)
O4–Cd3–O2#1	80.40(8)	N1–Cd3–O2#1	94.79(10)
N3–Cd3–O2#1	141.81(9)	O1#1–Cd3–O2#1	54.71(8)
N2–Cd3–O2#1	82.54(10)		
Complex **2**			
Co1–O3	2.059(5)	Co1–N1	2.099(5)
Co1–O1#1	2.107(6)	Co1–N4#2	2.113(6)
Co1–N2	2.156(6)	Co1–O2#1	2.271(17)
O3–Co1–N1	136.4(3)	O3–Co1–O1#1	133.5(3)
N1–Co1–O1#1	90.1(3)	N1–Co1–N4#2	92.5(2)
O1#1–Co1–N4#2	91.5(3)	O3–Co1–N2	85.8(2)
N1–Co1–N2	92.7(2)	O1#1–Co1–N2	89.9(3)
N4#2–Co1–N2	174.7(2)	O3–Co1–O2#2	79.0(4)
N1–Co1–O2#1	144.6(4)	O1#1–Co1–O2#1	54.6(4)
N4#2–Co1–O2#1	86.4(5)	N2–Co1–O2#1	90.2(5)
O3-Co1-N4#2	89.6(2)		
Complex **3**			

Cd1–N6	2.302(5)	Cd1–O6	2.350(5)
Cd1-N9#1	2.357(6)	Cd2–N2#2	2.294(5)
Cd1–O3	2.365(6)	Cd1–O9	2.390(5)
Cd1–O5	2.430(5)	Cd1–O4	2.443(5)
Cd2–O8	2.290(5)	Cd2–N4	2.369(6)
Cd2–O10	2.476(5)	Cd2–O7	2.590(5)
Cd2–O1#3	2.206(7)		
N6–Cd1–O6	91.60(19)	N6–Cd1–N9#1	172.9(2)
O6–Cd1–N9#1	93.1(2)	N6–Cd1–O3	84.7(2)
O6–Cd1–O3#3	169.04(15)	N9#1–Cd1–O3	89.8(2)
N6–Cd1–O9	88.95(18)	O6–Cd1–O9	87.44(19)
N9#1–Cd1–O9	85.9(2)	O3–Cd1–O9	82.21(19)
N6–Cd1–O5	86.88(19)	O6–Cd1–O5	53.87(15)
N9#1–Cd1–O5	100.2(2)	O3–Cd1–O5	135.87(17)
O9–Cd1–O5	140.88(19)	N6–Cd1–O4	95.4(2)
O6–Cd1–O4	137.61(17)	N9#1–Cd1–O4	84.7(2)
O3–Cd1–O4	53.20(17)	O9–Cd1–O4	134.3(2)
O5–Cd1–O4	84.79(16)	O1#3–Cd2–O8	166.4(2)
O1#1–Cd2–N2#2	100.2(3)	O8–Cd2–N2#2	86.1(2)
O1#3–Cd2–N4	84.5(3)	O8–Cd2–N4	92.3(2)
N2#2–Cd2–N4	165.36(17)	O1#3–Cd2–O10	100.3(3)
O8–Cd2–O10	92.1(2)	N2#2–Cd2–O10	84.5(2)
N4–Cd2–O10	81.0(2)	O1#3–Cd2–O7	113.9(2)
O8–Cd2–O7	52.59(17)	N2#2–Cd2–O7	106.2(2)
N4–Cd2–O7	84.1(2)	O10–Cd2–O7	141.0(2)

Symmetry transformations used to generate equivalent atoms: for **1**: #1 = 1+*x*, *y*, *z*. for **2**: #1 = -1+*x*, *y*, *z*; #2 = *x*, 1+*y*, *z*. for **3**: #1 = –1+*x*, *y*, –1+*z*; #2 = 1+*x*, *y*, –1+*z*; #3 = 1+*x*, –1+*y*, *z*.

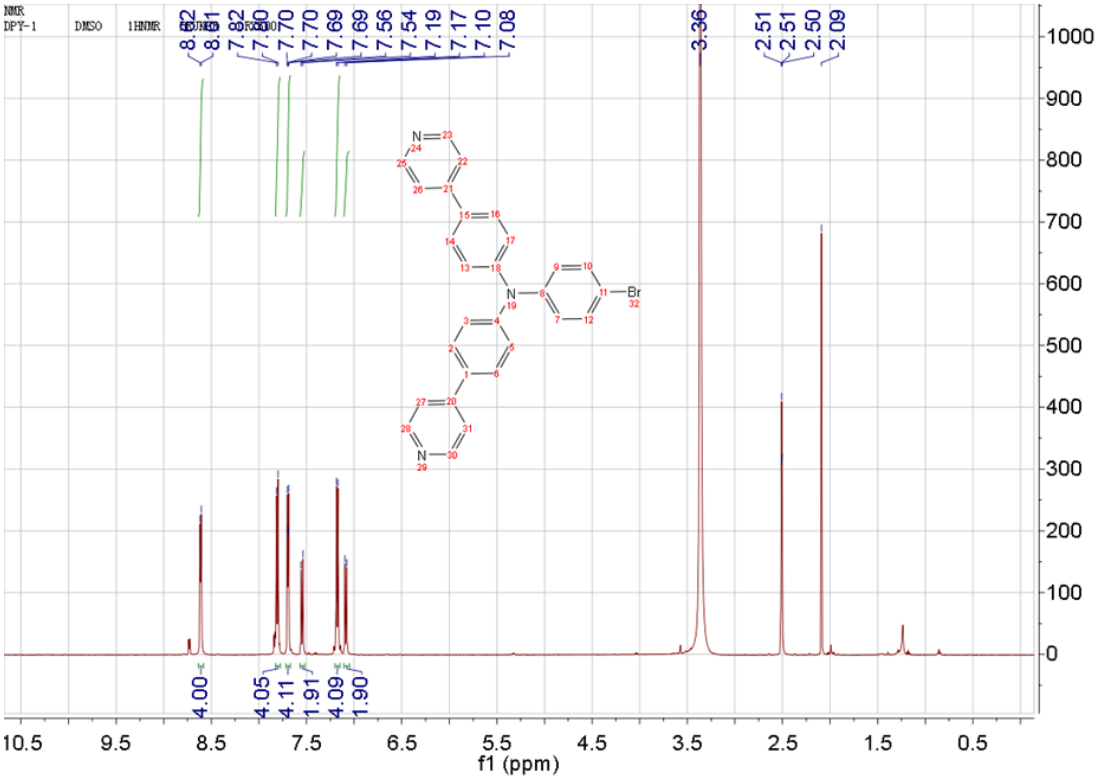

Fig. S1. ^{1}H NMR spectrum for I (DMSO–d_6, 500 MHz).

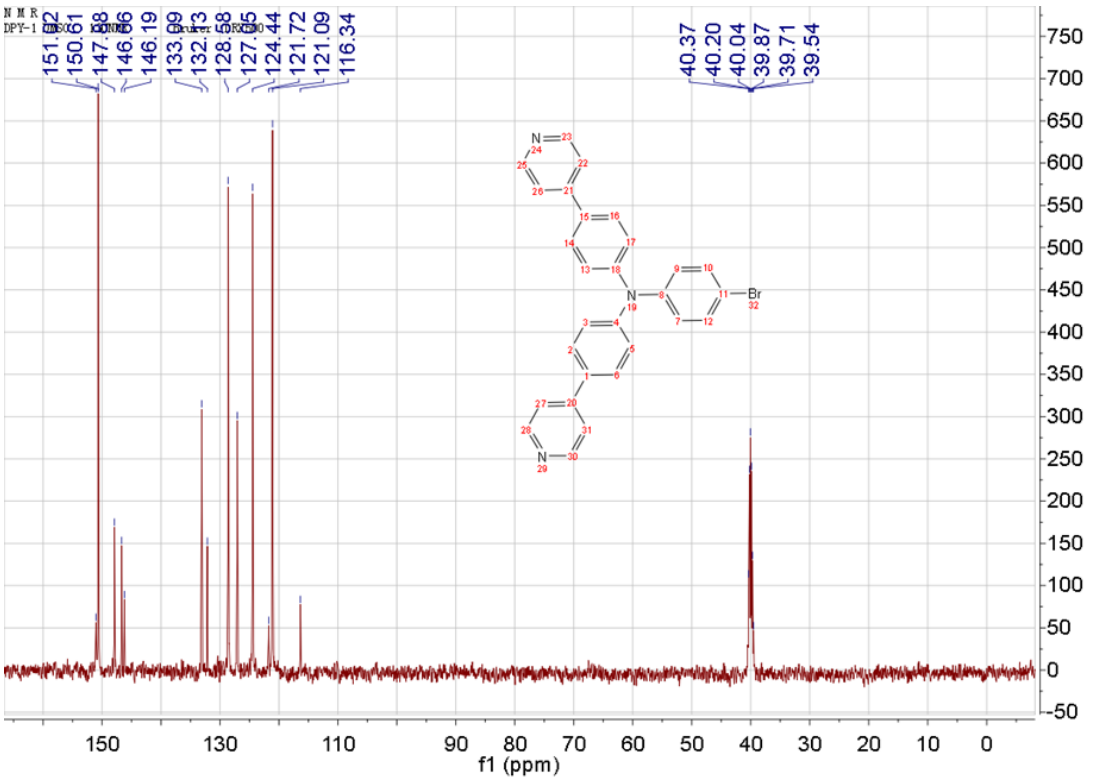

Fig. S2. ^{13}C NMR spectrum for I (DMSO–d_6, 125 MHz).

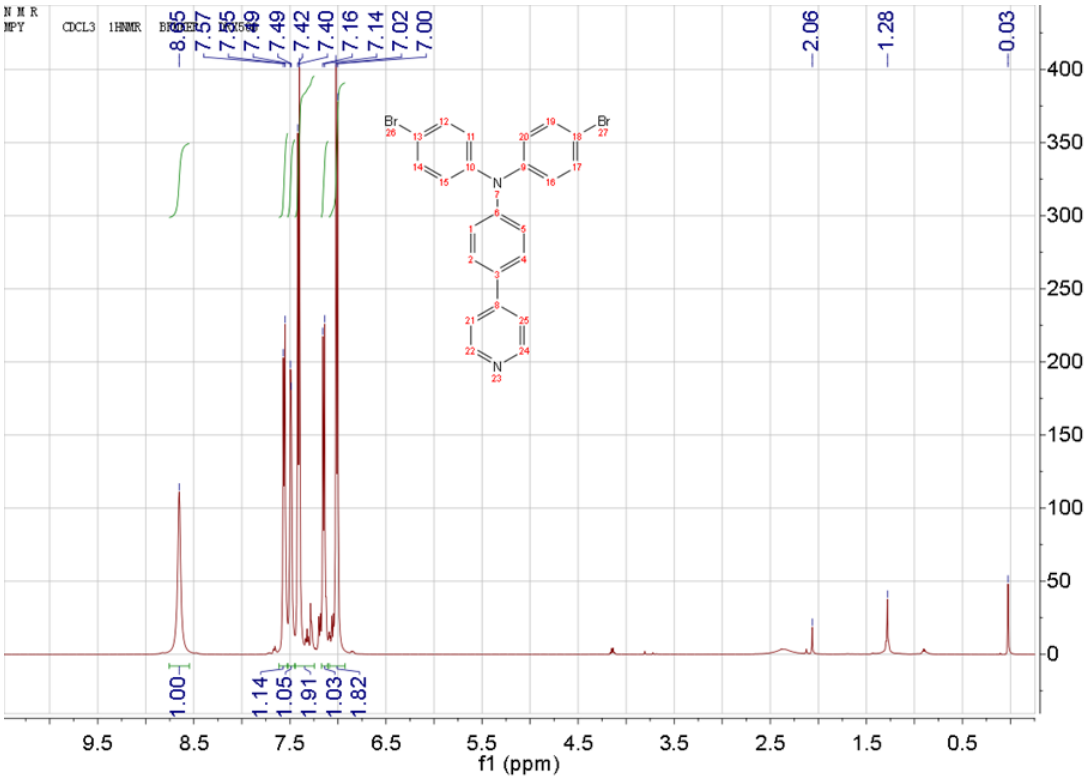

Fig. S3. ^{1}H NMR spectrum for II ($CDCl_3$, 500 MHz).

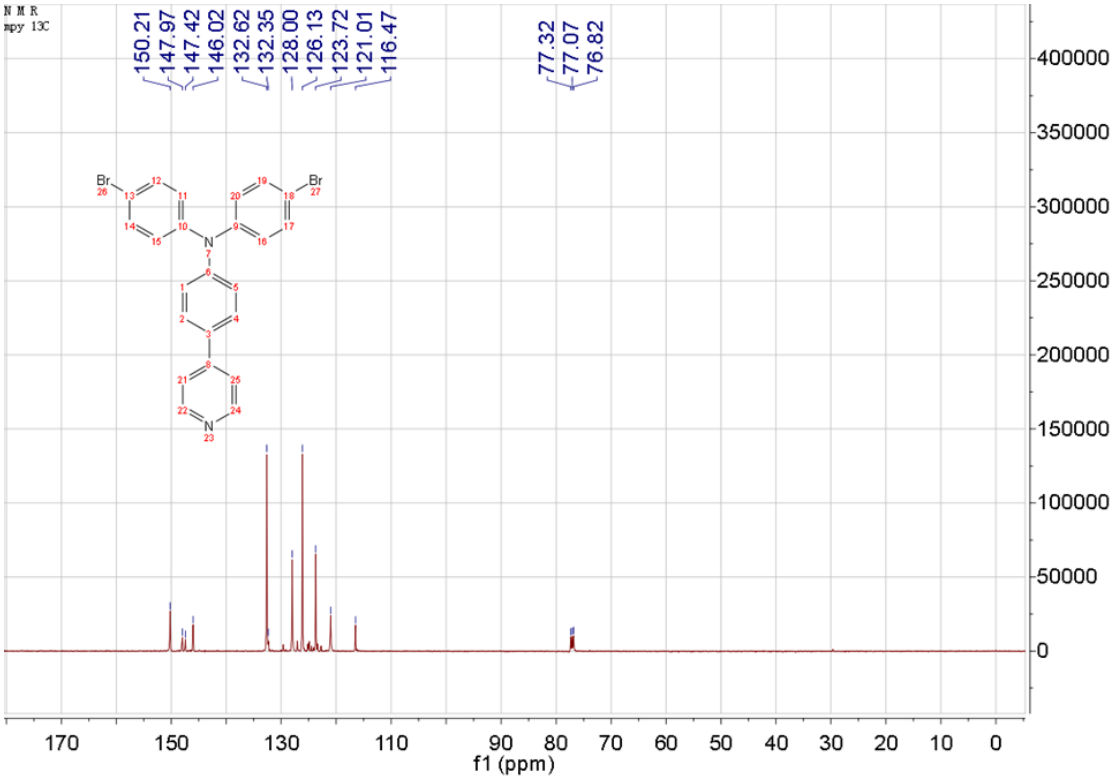

Fig. S4. ^{13}C NMR spectrum for II ($CDCl_3$, 125 MHz).

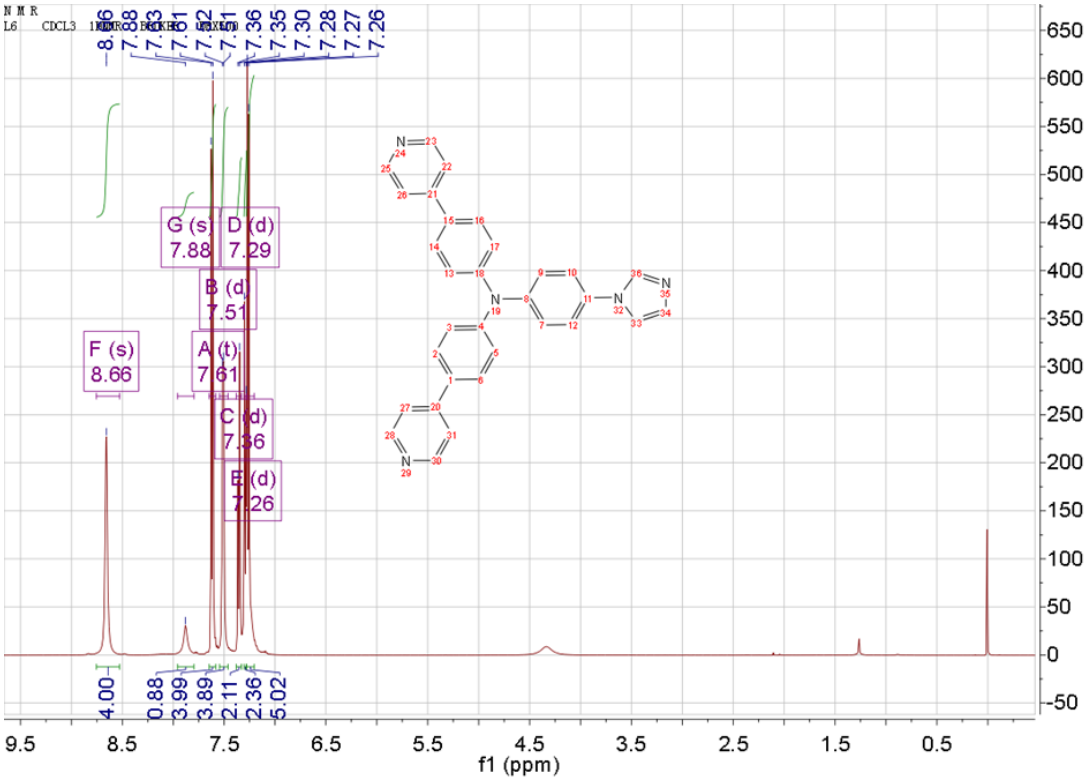

Fig. S5. ^{1}H NMR spectrum for MIDPPA ($CDCl_3$, 500 MHz).

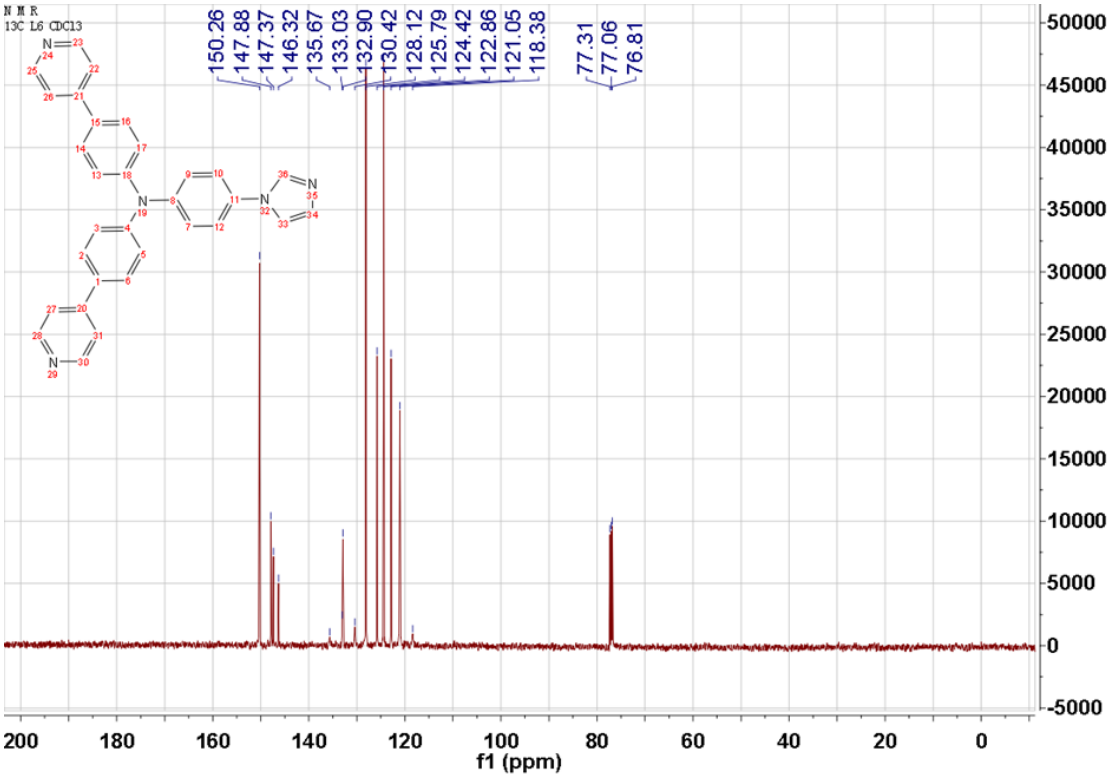

Fig. S6. ^{13}C NMR spectrum for MIDPPA ($CDCl_3$, 125 MHz).

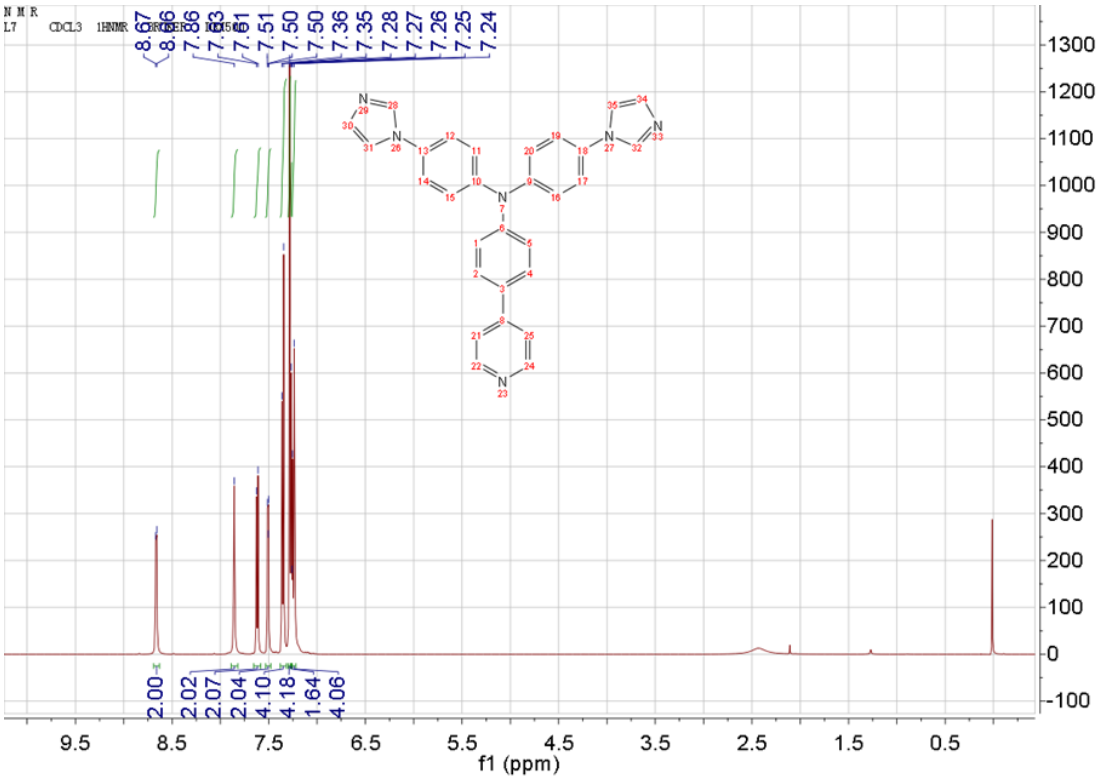

Fig. S7. ^{1}H NMR spectrum for DIMPPA ($CDCl_3$, 500 MHz).

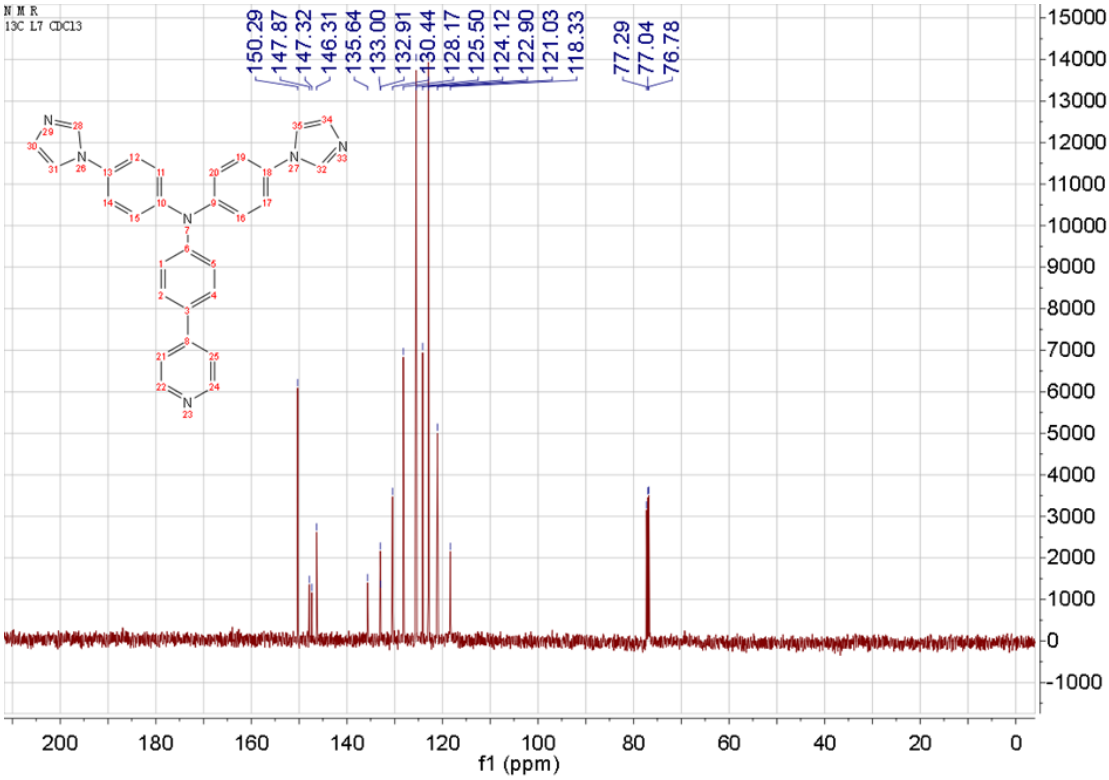

Fig. S8. ^{13}C NMR spectrum for DIMPPA ($CDCl_3$, 125 MHz).

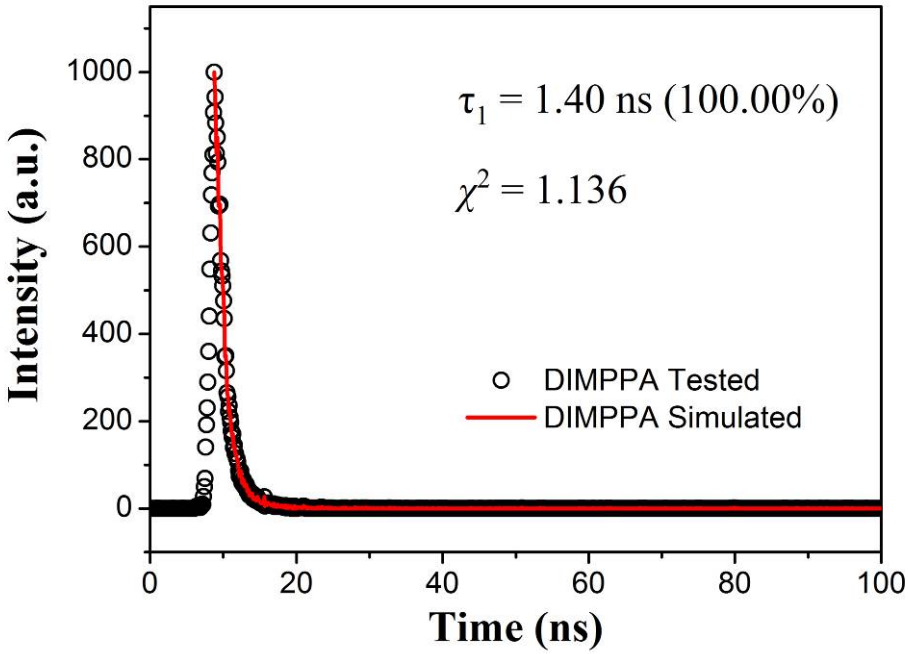

Fig. S9. The fitted decay curve monitored at 440 nm for free DIMPPA ligand in the solid state at room temperature. The sample was excited at 405 nm. Blank circles: experimental data; Solid line: fitted by Fit = A + $B_1 \times \exp(-t / \tau_1) + B_2 \times \exp(-t / \tau_2)$.

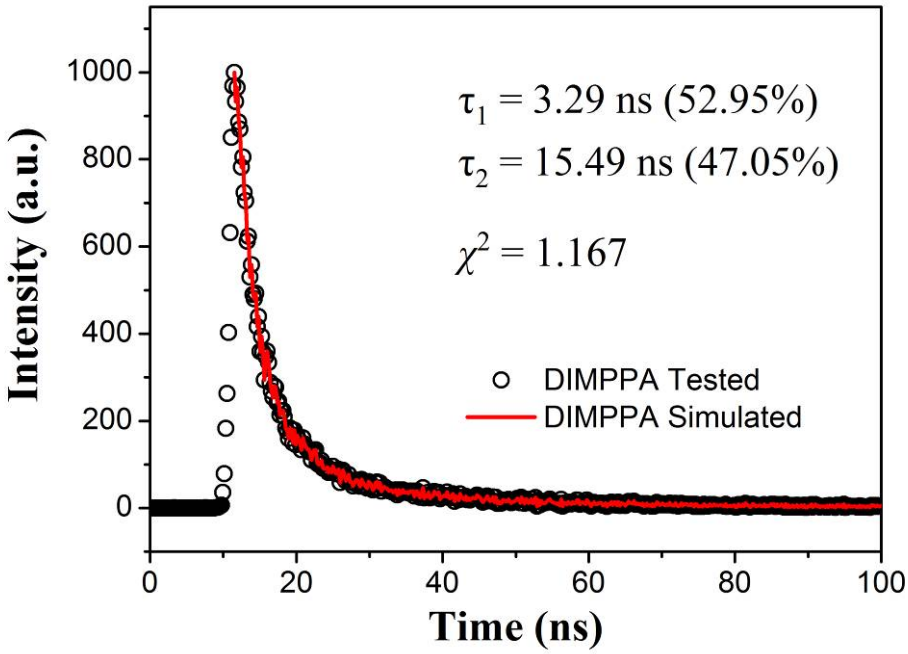

Fig. S10. The fitted decay curve monitored at 520 nm for free DIMPPA ligand in the solid state at room temperature. The sample was excited at 405 nm. Blank circles: experimental data; Solid line: fitted by Fit = A + $B_1 \times \exp(-t / \tau_1) + B_2 \times \exp(-t / \tau_2)$.

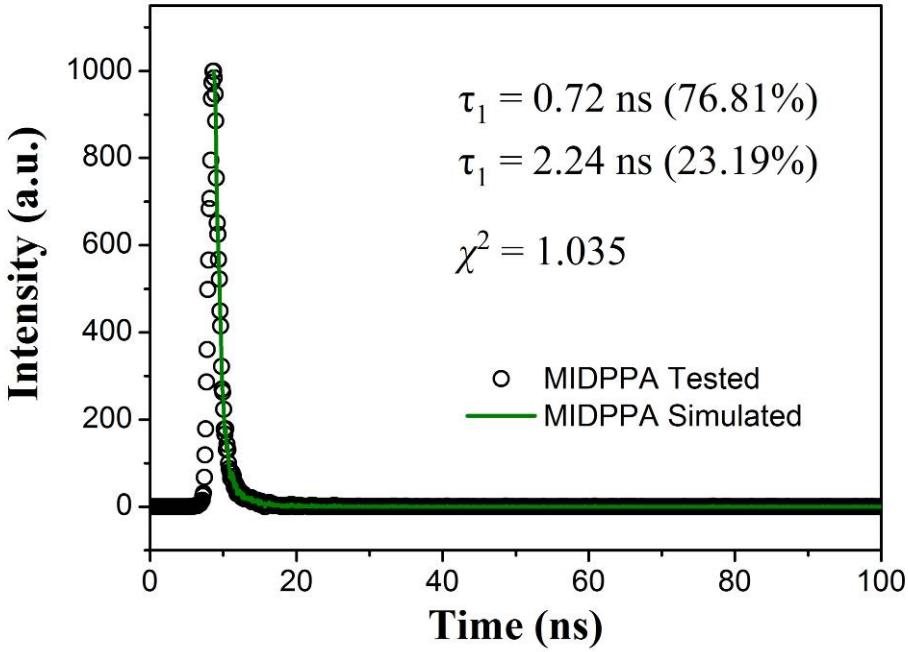

Fig. S11. The fitted decay curve monitored at 455 nm for free MIDPPA ligand in the solid state at room temperature. The sample was excited at 405 nm. Blank circles: experimental data; Solid line: fitted by Fit = $A + B_1 \times \exp(-t / \tau_1) + B_2 \times \exp(-t / \tau_2)$.

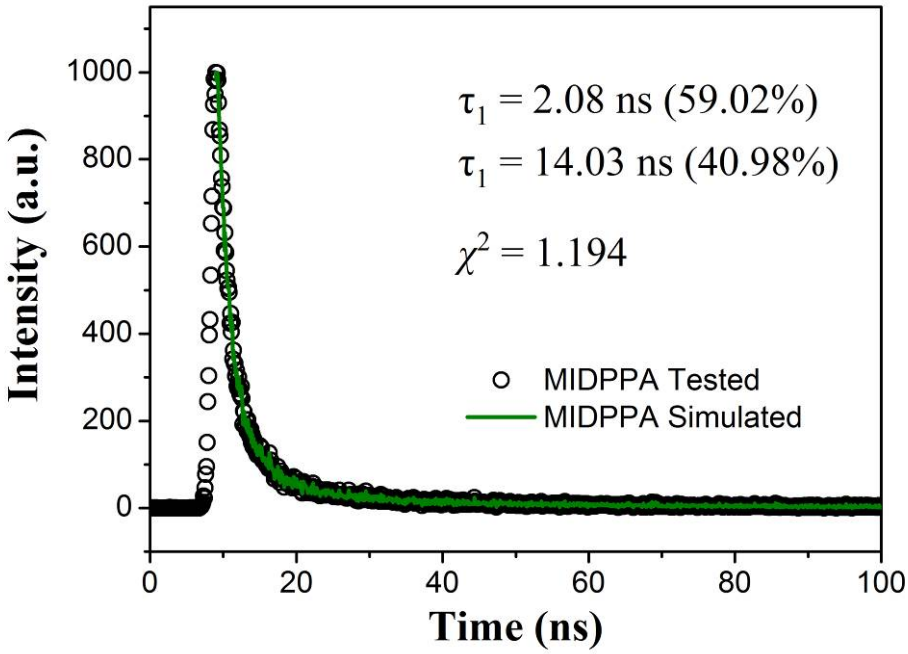

Fig. S12. The fitted decay curve monitored at 530 nm for free MIDPPA ligand in the solid state at room temperature. The sample was excited at 405 nm. Blank circles: experimental data; Solid line: fitted by Fit = $A + B_1 \times \exp(-t / \tau_1) + B_2 \times \exp(-t / \tau_2)$.

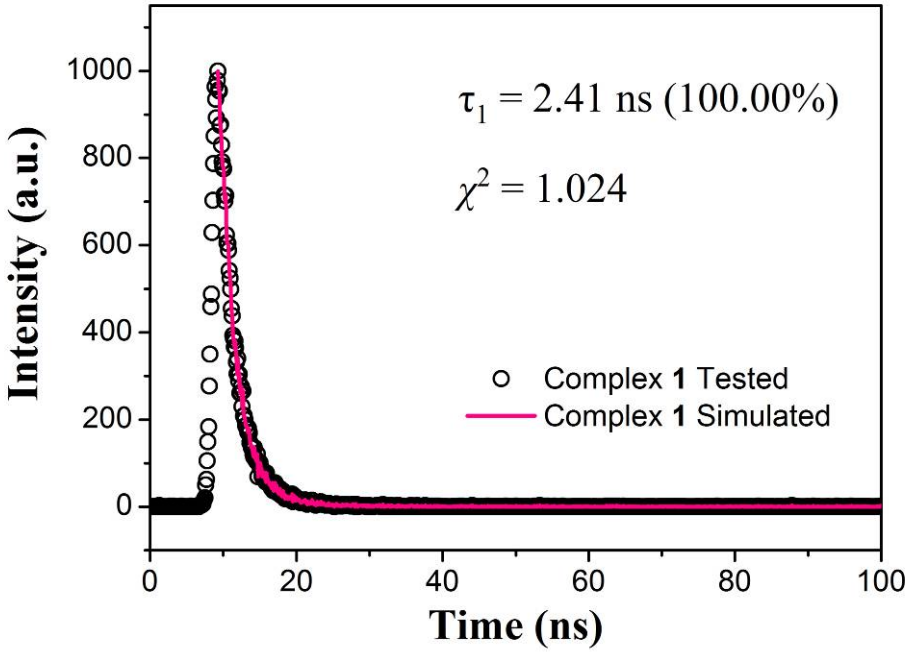

Fig. S13. The fitted decay curve monitored at 463 nm for complex **1** in the solid state at room temperature. The sample was excited at 405 nm. Blank circles: experimental data; Solid line: fitted by Fit = A + $B_1 \times \exp(-t / \tau_1) + B_2 \times \exp(-t / \tau_2)$.

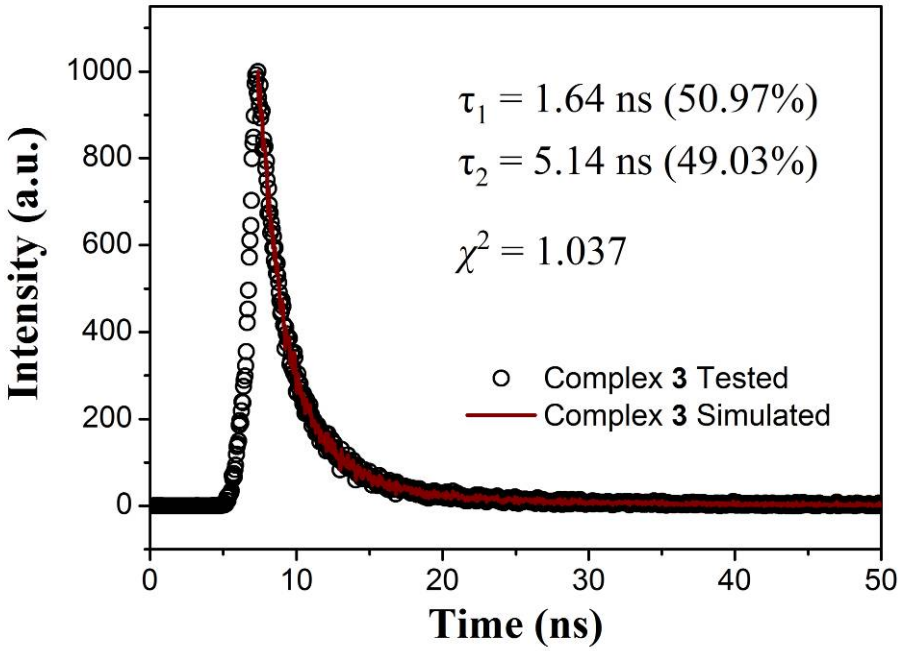

Fig. S14. The fitted decay curve monitored at 520 nm for complex **3** in the solid state at room temperature. The sample was excited at 405 nm. Blank circles: experimental data; Solid line: fitted by Fit = A + $B_1 \times \exp(-t / \tau_1) + B_2 \times \exp(-t / \tau_2)$.

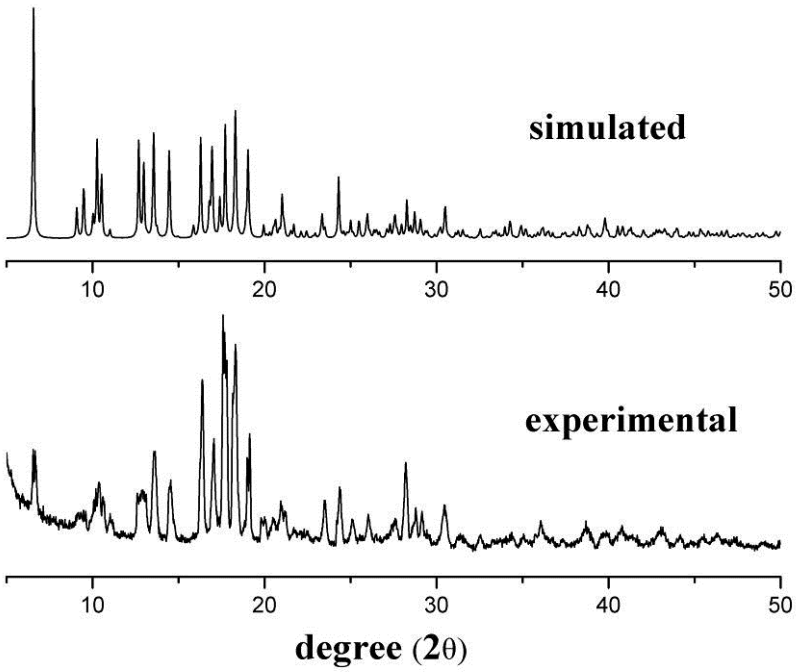

Fig. S15. PXRD plots of complex **1**.

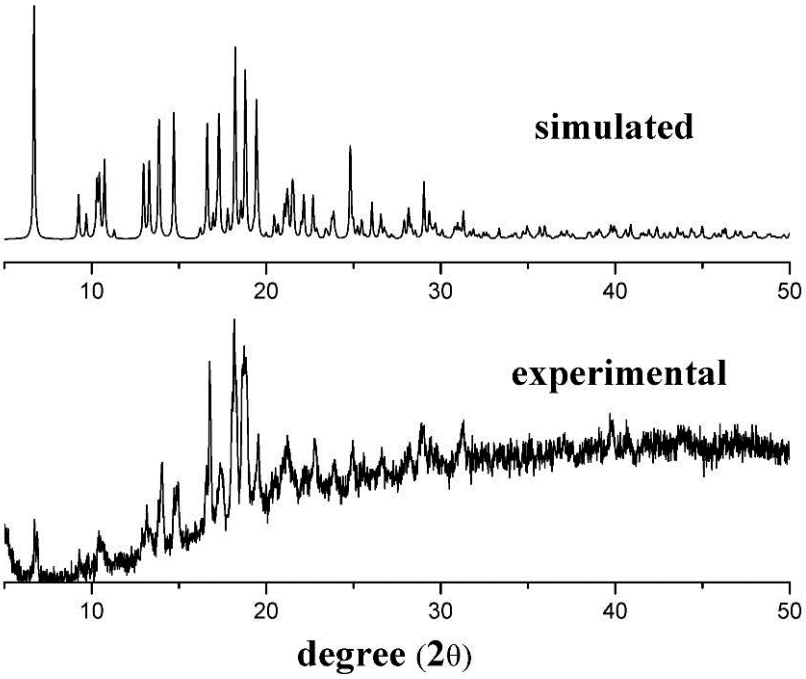

Fig. S16. PXRD plots of complex **2**.

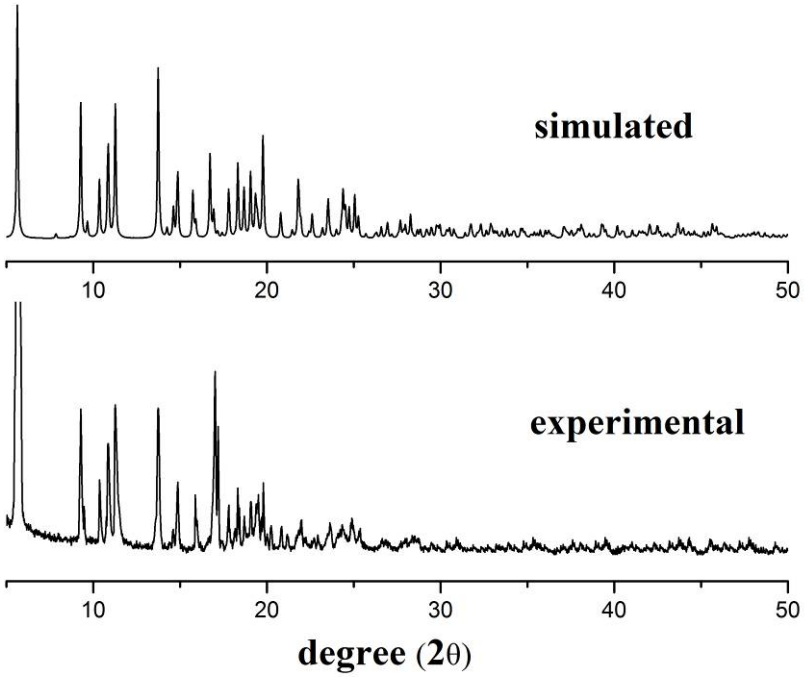

Fig. S17. PXRD plots of complex **3**.

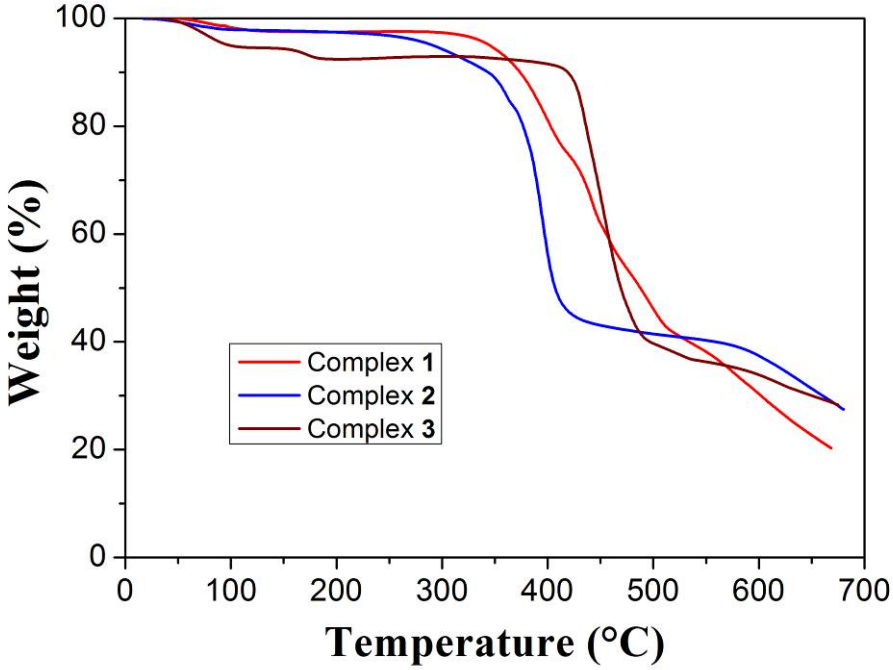

Fig. S18. Thermo-gravimetric plots of complexes **1-3**.